Comparison of different methods for simulating the behavior of laterally loaded piles

Alain Holeyman [a], *Anton Hübner* [b], *Helmut Saal* [b], *Olivier Tomboy* [a]

[a] Unité de Génie Civil et Environnemental
Université Catholique de Louvain
Louvain-la-Neuve, Belgium

[b] Lehrstuhl für Stahl- und Leichtmetallbau
Universität Karlsruhe (TH)
Karlsruhe, Germany

ABSTRACT

The behavior of laterally loaded piles is of significant interest for the load transfer in various constructions. Several methods are available for predicting the lateral behavior of piles in cohesionless soil. In this paper, the three main approaches are applied and compared for a reference case, i.e. the well-known approach using *p-y* curves, the elastic continuum theory and more detailed numerical finite element analyses. Two types of design procedures were used to evaluate the parameters of the different methods. It is concluded that methods using the same calibration strategy provide similar results. However, the calibration of the elastic parameters based on laboratory tests and more particularly triaxial tests seem to give softer behavior of the soil compared to the more empirical solutions.

KEY WORDS: pile, lateral, cohesionless, soil, FE, hypoplasticity.

NOMENCLATURE

A, A_R	empirical correction factor	[-]
c'	effective cohesion	[kPa]
C_1, C_2, C_3	coefficients	[-]
C_u	coefficient of uniformity	[-]
D	pile diameter	[m]
d_{50}	mean diameter of the grain	[mm]
E	Young's modulus of the soil	[MPa]
E^{50}	Young's modulus of the soil at 50 % of the failure load from triaxial tests	[MPa]
E_s	soil modulus (1D model)	[MPa]
E_pI_p	flexural stiffness of the pile	[MNm²]
e, $e_{0,ini}$	void ratio, initial void ratio	[-]
e_{d0}, e_{c0}, e_{i0}	minimum, critical and maximum void ratio for a stress-free state (hypoplasticity)	[-]
e_{max}, e_{min}	maximum and minimum void ratios	[-]
h_s	granular stiffness (hypoplasticity)	[MPa]
k_i	initial stiffness	[MN/m³]
K_0	earth pressure coefficient at rest	[-]
n	exponent (hypoplasticity)	[-]
n_h	constant of horizontal subgrade reaction	[MN/m³]
p	lateral soil reaction or resistance	[kN/m]
t	shell thickness	[m]
y	pile deflection	[m]
z	depth	[m]
α, β	exponents (hypoplasticity)	[-]
γ, γ', γ_{min}, γ_{max}, γ_s	density for different states	[kN/m³]
δ	angle of interface friction	[°]
φ'	effective angle of internal friction	[°]
μ	Poisson ratio	[-]
ν	dilation angle	[°]
σ, $\boldsymbol{\sigma}$	normal stresses, stress tensor	[kPa]
σ_m	mean pressure	[kPa]
τ	shear stresses	[kPa]

INTRODUCTION

Piles are used in different constructions e.g. monopiles in offshore engineering, combiwalls in harbor constructions, or piles and column foundations. In this context the piles are subjected to lateral loads and thus the understanding of the lateral behavior of these piles is substantial for the design of such structures.

Several methods are available for predicting the lateral behavior of piles in cohesionless soil. The subgrade reaction approach using a series of uncoupled discrete springs is probably the simplest method for modeling the pile-soil interaction. The most complex method of taking the interaction into account arises from modeling not only the structure itself but also the soil as a three-dimensional body. This approach involves the modeling not only of the soil and the pile but also of the contact between the two components. This more detailed analysis accounts for (1) spatial load transfer mechanisms, that cannot be covered by the subgrade reaction approach, and (2) mechanically more consistent soil properties. In an investigation with a three-dimensional model for the continuum, different material models can be used (e.g. linear elastic continuum, Mohr-Coulomb plastic material, hypoplastic model).

The three commonly used approaches which are discussed within this paper are the approach using p-y curves, elastic continuum theory, and numerical finite element analyses involving more detailed soil models. Even though the first two methods are still widely used in the practical design of laterally loaded piles, they suffer from some shortcomings. The linear elastic continuum theory does not capture the nonlinearity of the problem, and the *p-y* curves use nonlinear transfer curves derived from experiments that cannot be easily adapted to different situations. However, nonlinear finite element analyses provide potentially superior and flexible tools to cope with these shortcomings.

APPROACHES FOR MODELLING THE SOIL-PILE INTERACTION

The Subgrade Reaction Method with *p-y* Curves

The Winkler approach (1867) is the oldest method for modeling soil and soil-structure interaction in simple applications. In this approach, also called subgrade reaction theory, the soil is modeled by a series of uncoupled discrete linear springs with a stiffness E_s (= soil modulus) expressed in f/l^2 [*force/length*^{2}]. For piles the soil modulus E_s represents the ratio between the lateral soil reaction p [f/l] and the pile deflection y [l]. For piles embedded in sand it is common to assume that E_s varies linearly with depth and Terzaghi's recommendations (Terzaghi, 1955) are generally adopted:

$$E_s = \frac{p}{y} = n_h \cdot z \tag{1}$$

where n_h is the constant of horizontal subgrade reaction expressed in f/l^3 (see Table 1), and z the depth below the ground line.

Table 1. Constant n_h of lateral subgrade reaction for sand (after Terzaghi, 1955)

relative density	loose < 35 %	medium	dense > 65 %
n_h (MN/m³)	2.2	6.6	18

The lateral pile behavior is described by the following governing equation originally presented by Hetenyi (1946) :

$$E_p I_p \frac{d^4 y}{dz^4} + p = 0 \tag{2}$$

in which $E_p I_p$ is the flexural stiffness of the pile. McClelland and Focht (1956) initially extended the subgrade reaction approach using the finite difference technique to account for non-linear soil reaction versus deflection relationships (Fig. 1). Their approach is known as the *p-y* method.

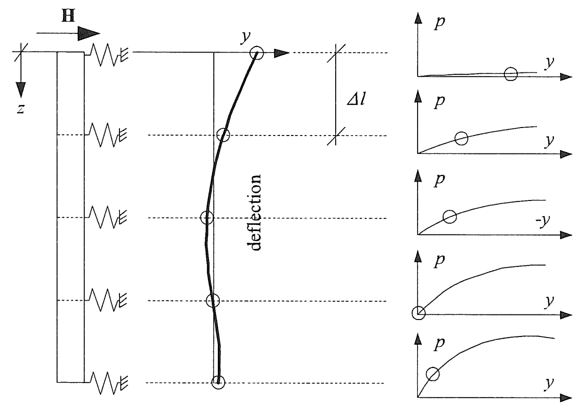

Fig. 1. p-y curves concept for an embedded pile

Based on field load tests, Reese et al. (1974) derived empirical *p-y* curves for sands. Their *p-y* curves are based on linear and parabolic functions defined for segments. The parameters for each function are given by the effective angle of internal friction φ' and the initial stiffness $E_{s,i}$ [f/l^2] expressed as $k_i \cdot z$.

A more detailed approach given by Reese et al. (1974) uses two simplified spatial soil failure models to compute the ultimate lateral resistance $p_u(z)$ of a pile with diameter D: (1) a wedge failure mechanism near the soil surface where the self-weight of the wedge of soil represents the soil resistance p_{st} and (2) a plastic flow failure at greater depths where the soil resistance p_{sd} is computed under plane strain conditions with the Mohr-Coulomb failure criterion. The ultimate lateral resistance $p_u(z)$ is defined as the minimum of p_{st} and p_{sd} multiplied by an empirical factor $A_R(z)$:

$$p_u(z) = A_R(z) \cdot min\{p_{st}(z), p_{sd}(z)\} \tag{3}$$

Details on the evaluation of the curve segments are for example given in Reese et al. (1974), Reese and Van Impe (2001), and Wiemann et al. (2004). The procedure by Reese et al. (1974) for constructing the *p-y* curves for sands is commonly used and therefore implemented in several commercial packages as e.g. LPILE®. However, for the design procedure the concept was simplified. In more recent guidelines as for example the "Det Norske Veritas" (2004) and "ISO/DIS 19902" (2004) the *p-y* curves for sand are described with continuous hyperbolic tangent functions:

$$p(y,z) = p_u(z)\, tanh\left(\frac{k_i\, z}{p_u(z)}\, y\right) \tag{4}$$

The limitation of the lateral stresses in the soil for static loads by the soil resistance $p_u(z)$ [f/l] is given in a simple manner for all cases :

$$p_u(z) = A(z) \cdot min \begin{Bmatrix} \gamma'\, z^2\, C_1 + \gamma'\, z\, C_2\, D \\ \gamma'\, z\, C_3 \end{Bmatrix} \tag{5}$$

where $A(z)$ is an empirical correction factor, γ' the soil's effective unit weight, while the coefficients C_1, C_2, and C_3 are correlated with the effective friction angle of the soil φ'. The value for the initial stiffness k_i [f/l^3] can also be determined as a function of the effective friction angle φ'. For a more detailed description of the procedure see Wiemann et al. (2002).

Elastic Continuum Theory

Besides modeling the soil with springs it can be defined in a first approach as a linear elastic and homogenous continuum for overcoming e.g. the lack of load spreading given by the Winkler spring model (discrete formulation). The simplest approach is to use a linear elastic material model which involves the parameters Young's modulus E and Poisson ratio μ. For analyzing this approach a pile entirely connected to an elastic continuum can be investigated. The homogenous linear elastic assumption allows analytical solutions using Mindlin's closed form solutions for the soil displacement due to a point load embedded in a semi-infinite medium (Poulos, 1971). Subsequent enhancements of the theory deal with the accounting for (1) a yielding limit, (2) a pile-soil separation and (3) a varying soil modulus with depth (Poulos, 1980). However, even if the theory is very convenient for practical use, it does not capture the real soil behavior and the pile soil separation is very complicated to be tackled.
In this paper, the elastic continuum approach has been considered from the aspect of numerical analysis. For numerical analyses the computational power allows the user to work with complex three-dimensional problems involving the modeling of the soil using a material model and a specific contact definition.

Since this problem also affects the complex finite elements with more elaborate material models this aspect is discussed in the corresponding subsection.

Detailed Numerical Finite Element Analyses

Nonlinear Material Models

3-D finite element methods using the FEM package ABAQUS® are used in order to give a reasonably realistic model, accounting for the spatial effect of a single laterally loaded pile. The model involves detailed constitutive soil models and a soil-structure interaction with possible pile-soil separation during loading. The investigated constitutive soil models include (1) a classical elasto-plastic model with a Mohr-Coulomb yield surface and non-associated flow rule and (2) a more elaborate hypoplastic model.
The basis for the first soil model is to assume linear elasticity. The Mohr-Coulomb plasticity is a common failure criterion encountered in geotechnical engineering. The Mohr-Coulomb criterion describes a linear relationship between normal effective stresses σ' and shear stresses τ on the failure plane:

$$\tau = c' + \sigma' \tan\varphi' \qquad (6)$$

in which c' is the effective cohesion of the material and φ' the effective angle of friction of the material. The used Mohr-Coulomb model has a smooth flow potential function (hyperbola) characterized by the dilation angle ν. The model is applied with a non-associated flow rule and no hardening.
It is commonly recognized that for geomaterials the assumption of bilinear response proposed in elasto-plastic models is inexact. The hypoplasticity was introduced to describe the soil as highly non-linear and inelastic by taking into account, amongst others, the distinct change of volume under shear deformation. Based on the theory of Truesdell (1955) a new formulation was derived, which advanced significantly over the years (Darve, 1974; Chambon and Renoud-Lias, 1979; Kolymbas, 1988; Bauer, 1996; Gudehus, 1996; Bauer and Herle, 2000). The formulation embeds the elastic and the plastic behaviors into a single incremental equation.

$$\dot{\sigma} = \dot{\sigma}\left(\sigma, e, \dot{\varepsilon}\right) \qquad (7)$$

where $\dot{\sigma}$ is the stress increment, $\dot{\varepsilon}$ is the current strain increment, σ is the current stress, and e is the void ratio.
The recent development in the field of hypoplasticity allows a relatively simple modeling of the soil in comparison to the previous approaches to be implemented in standard finite element programs. The hypoplasticity formulation implemented by Nübel and Niemunis (1999) as a FORTRAN® routine in ABAQUS® was used for the analyses.

Contact between Pile and Soil

One of the important issues for simulating pile behavior is the correct modeling of the thin zone at the interface between soil and pile. For laterally loaded piles, this zone is subjected to frictional behavior with a possible gap due to lateral displacement, removing all transmission of the stress between soil and pile. "Surface-to-surface" contact as defined in the ABAQUS® jargon using augmented Lagrange formulation and allowing separation after contact was applied for the investigated case. Based on the suggested values of Khulaway (1991) for smooth steel piles, an angle of interface friction $\delta = 0.5\varphi'$ is introduced by working with a Coulomb friction law.

ANALYSES AND COMPARISON

Reference case

A reference case based on an experimental test set-up developed in the Civil Engineering laboratory at the Université catholique de Louvain is calculated using the different approaches. Similar comparisons for the field of offshore wind energy structures have been performed i.e. by Wiemann et al. (2004), Dalhoff and Taferner (2003), and Grabe et al. (2005).
A 3 m long steel tube with an external diameter of D = 200 mm and a thickness t = 2 mm which is vertically embedded in dry sand is chosen as reference case (Fig. 2). The choice of geometry and system is made in accordance with the experimental part of the investigations referenced in the Acknowledgments section. Details on the test set-up are given in a companion paper (Charue et al., 2006). The modeled tube is positioned vertically in a cylindrical casing with a diameter of 30D (6 m) and subsequently embedded in dry sand. A large casing was chosen for the numerical investigation in order to be able to compare the results from the 3-D analyses with the p-y calculations which are based on empirical findings. Preliminary finite element analyses revealed a negligible influence of the boundary effects for the proposed diameter of the casing. The pile head is loaded with a horizontal load of 10 kN corresponding to a factor of safety of approximately 1.4. In this study the vertical displacement of the pile head is restrained. The boundary conditions are shown in Fig. 2.

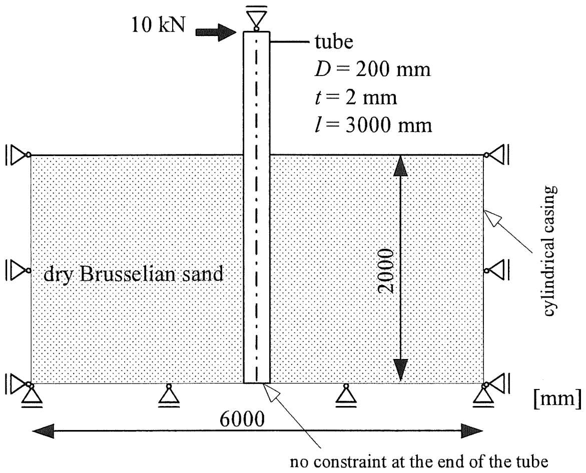

Fig. 2. Cross-section of the reference case with applied boundary conditions

"Brusselian Sand" is used for the study. This sand was thoroughly investigated in Louvain-la-Neuve (Vanden Berghe, 2001) by numerical and experimental means. The physical characteristics of the sand are summarized in Table 2. Following the ASTM Standard D-2487, the sand is classified as poorly graded (SP). The sand is assumed to be pluviated to an initial void ratio of 0.7 (γ = 15.25 kN/m³), allowing geostatic stress condition to develop, with a K_0 value of 0.46.

Table 2. Physical parameters of the "Brusselian Sand"

d_{50} [mm]	$C_u(= d_{60}/d_{10})$ [-]	γ_{min} [kN/m³]	γ_{max} [kN/m³]	γ_s [kN/m³]	e_{max} [-]	e_{min} [-]
0.18	2.2	11.91	17.09	25.97	1.18	0.52

Consistent Soil Data

A set of consistent constitutive parameters for the modeled sand is first derived using experimental data from previous laboratory investigations (triaxial and oedometer tests) performed by Vanden Berghe (2001). Table 3 summarizes the investigated material models, the soil properties, and defines the soil parameters to be used for the corresponding approach. Table 4 lists the additional parameters required by the hypoplastic model.

Table 3. Material properties for the "Brusselian Sand" according to the different approaches

approach	Terzaghi	*p-y* according to Reese et al. 1974	*p-y* with hyperbolic function – ISO/DIS	linear Elastic medium	elasto-plastic MC FEM	hypoplasticity FEM
γ' [kN/m^3]	*NA*	15.25	15.25	15.25	15.25	15.25
φ' [°]	*NA*	33	33	*NA*	33	33
c'[kPa]	*NA*	0	0	*NA*	0.2$^{\#}$	0.2$^{\#}$
k_i [MN/m^3]	6.6$^{\#\#}$	24.4	17.6	*NA*	*NA*	*NA*
E [MPa]	*NA*	*NA*	*NA*	2.35	4.4	NA
μ [-]	*NA*	*NA*	*NA*	0.35	0.35	NA
ν [°]	*NA*	*NA*	*NA*	*NA*	6	NA

$^{\#}$ = *improves numerical convergence*
$^{\#\#}$ = *secant stiffness at working load*
NA = not applicable

Table 4. Additional material properties for the "Brusselian Sand" according to the hypoplastic model (after Vanden Berghe, 2001)

e_{d0} [-]	e_{c0} [-]	e_{i0} [-]	n [-]	α [-]	β [-]	h_s [MPa]
0.52	0.88	1.21	0.35	0.3	1.1	200

Based on a series of triaxial tests, the strength parameters φ' and c' are well defined and equal to 33° and 0 kPa, respectively (Fig. 3). However, for the analyses using the Mohr-Coulomb failure criterion and the hypoplastic material a small cohesion c' of 0.2 kPa is applied to improve numerical stability.

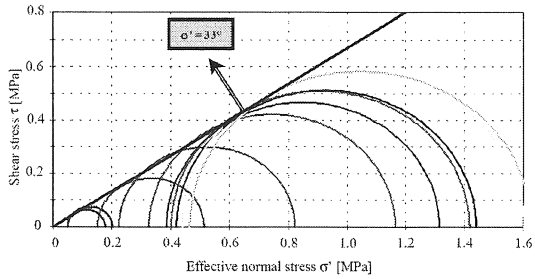

Fig. 3. Mohr's Circle deduced from drained and undrained monotonic triaxial tests on "Brusselian sand" with $e = 0.7$ (after Vanden Berghe, 2001)

Subgrade reaction approach

For the *p-y* methods the guidelines issued from the literature and representing the engineering practice have been followed (Terzaghi, 1955; Reese et al., 1974; ISO/DIS 19902, 2004). As previously reminded only the effective angle of internal friction φ' of the sand and the (initial) stiffness k_i have to be determined. According to the considered method, the latter parameter can be expressed either as a function of φ' or as a function of the relative density of the sand. Based on a value of 33° for φ', the sand is assumed to be installed with a medium relative density as recommended by *API* (1994). It should be emphasized that the stiffness k_i represents an initial stiffness for the *p-y* procedure while it corresponds to a secant stiffness under working load conditions for the Terzaghi procedure.

Hypoplastic model

The hypoplastic parameters (Tables 3 and 4) were derived by Vanden Berghe (2001) according to the calibration procedure proposed by Bauer (1996) and Herle and Gudehus (1999). Vanden Berghe (2001) however used data from an oedometric compression in lieu of an isotropic oedometric compression to derive the parameter β governing the soil's stiffness. The simulated response of soil with hypoplastic model depends highly on the initial conditions. In the current study, the initial void ratio e_0 has been assumed equal to 0.7. For an initial void ratio of 0.7, the hypoplastic parameters presented in Tables 3 and 4 lead to an effective friction angle φ' of 33°.

Elastic model

For the homogeneous elastic model, the strategy adopted in this investigation consists in deriving a constant Young's modulus E from Terzaghi's empirical recommendations for the soil modulus E_s.
Based on 2-D plane strain system with a rigid cylinder displaced laterally in an homogenous elastic medium characterized by a Young's modulus E and a Poisson ratio $\mu = 0.33$, Baguelin et al. (1977) proposed the following relationship to derive the soil modulus E_s as defined by Eq. 1:

$$E_s = \frac{E}{0.808 + 0.265\, ln \dfrac{R}{30 r_0}} \tag{8}$$

where R is the outside radius of the model and r_0 is the pile radius.
For the reference case, the Terzaghi's recommendations for medium sand involve a soil modulus E_s value varying from 0 MPa at the ground line to 13.2 MPa at 2 m depth (Eq. 1 and Table 1). An equivalent soil modulus E_s for a homogeneous medium (constant with depth) had to be calculated first. This preliminary study revealed that similar pile head deflection was obtained considering a constant soil modulus E_s of 2.9 MPa emphasizing the importance of the stiffness of the layers near the ground surface. Considering this value of 2.9 MPa, Eq. 8 leads for the reference case ($R = 30r_0$) to a Young's modulus E of 2.35 MPa.

Elasto-plastic models

The elasto-plastic model requires also the definition of a Young's modulus expressing the elastic soil behavior before plastic flow. The strategy consisting in evaluating the secant Young's modulus E^{50} at 50 % of the failure load from triaxial tests has been adopted to that end (Fig. 4). However, while the strength parameters are easily evaluated for the elasto-plastic model, the calibration of the elastic parameters appears more complex due to their stress level dependency.

The behavior of laterally loaded piles is mainly governed by the soil layers near the ground surface where very small confining pressures develop. Before lateral loading, the mean pressure σ_m (Eq. 9) in the soil under geostatic conditions ranges from 0 kPa to 20 kPa in the depth range 0 m < z < 2 m, with σ_m defined as:

$$\sigma_m = \frac{1}{3}(\sigma_1 + \sigma_2 + \sigma_3) \tag{9}$$

in which σ_i are the principal stresses.

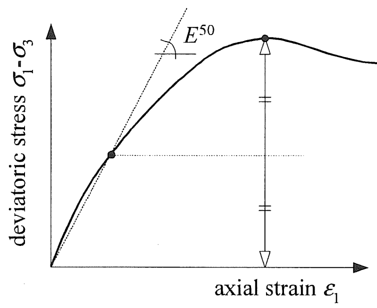

Fig. 4. Definition of Young's modulus at 50 % of the failure load E^{50} from triaxial tests

After lateral pile loading, this pressure increases up to 100 kPa in the region of maximum mean pressure at 0.5 m depth. Unfortunately, little laboratory investigation on the Brusselian sand has been carried out under confining pressures of about 100 kPa. That is why a stress dependent power function was used to approximate the sand secant Young's modulus E^{50}, as shown in Fig. 5, according to:

$$E^{50} = E^{50}_{ref}\left(\frac{\sigma_m}{\sigma_{ref}}\right)^m \tag{10}$$

with E^{50}_{ref} = 22 MPa, σ_{ref} = 100 kPa, and m = 0.7.

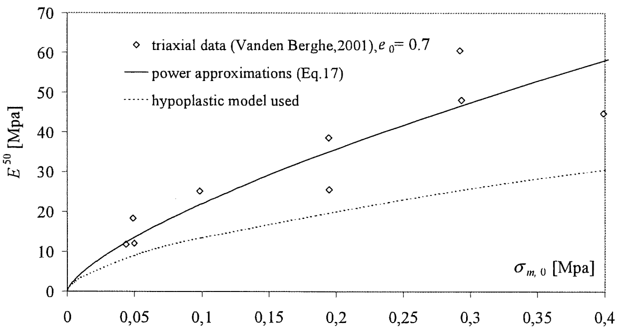

Fig. 5. Evaluation of Young's modulus at 50 % of the failure load from triaxial tests as a function of the initial mean pressure

The secant Young's modulus E^{50} was estimated from the triaxial data and plotted against the initial mean pressure $\sigma_{m,0}$.
Analyzing the different stress intervals results in different moduli for each interval. As an approximation for the reference case, it is chosen to adopt for the elasto-plastic model $E = E^{50}$ = 4.4 MPa corresponding to an average mean pressure of 10 kPa before loading.

The evaluation of the angle of dilation ν for the numerical analyses using an elasto-plastic material model with Mohr-Coulomb failure criterion is based on the results from studies with the hypoplastic material model. In a study the angle of dilation for the elasto-plastic model is varied in numerical simulations of drained triaxial compression tests. The comparison of volume changes indicates that an angle of dilation $\nu = 6°$ can be used as an approximation.

As a conclusion, two broad categories of design procedures have been used: (a) design in which the parameters were evaluated based on empirical relationships for cohesionless sand including the 1-D approaches and the 3-D approach with the elastic model and (b) design in which the parameters were calibrated based on laboratory investigations on Brusselian sand including the 3-D approaches using the elasto-plastic and hypoplastic models.

Calculations and Results

The mesh size used for finite element simulations is based on a preliminary convergence study with a fine mesh close to the pile and a coarser mesh further away from the pile. The modeling of the tube and the soil is performed with linear isoparametric elements (Hibbit et al., 2005).
For all numerical simulations, the initial conditions consisted of a self-equilibrating geostatic stress field with a weightless pile and an earth pressure coefficient K_0 at rest of 0.46 (= 1-$sin\varphi'$). Subsequent loading was then incrementally applied on the pile head. For the different approaches, Table 5 summarizes the results in terms of displacements.

In order to test the validity of the three-dimensional model an analytical solution based on Mindlin's closed form solution considering Young's modulus of 2.35 MPa has been calculated. Midlin's solution assumes that the soil is entirely connected to the pile during the loading. Including similar assumptions in the finite element model, the pile's lateral displacement at ground line for a lateral load of 10 kN is 1.0 cm while the analytical solutions reaches 1.3 cm. The difference between these values may come from prescribing the boundary conditions in the finite element model while the analytical solution assumes a semi-infinite medium leading consequently to a larger displacement. However, it is supposed that the correspondence is sufficient to validate the finite element model.

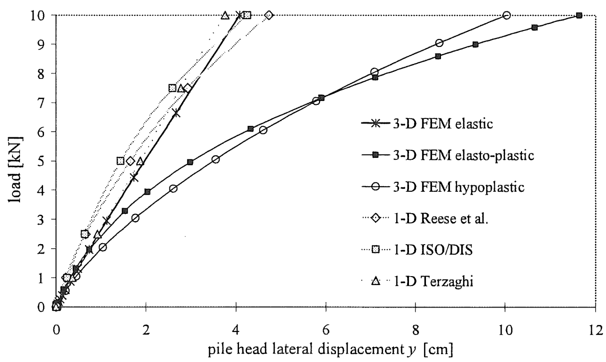

Fig. 6. Pile head deflection comparison for all the methods

The load-deflection curves for the pile as a result of the different analyses are compared in Fig. 6 while Fig. 7 shows the pile deflection distribution along the depth. Fig. 8 depicts the deformed system for the hypoplastic analysis. According to the adopted calibration procedure for soil parameters and interface parameters, good agreement can be observed between the different 1-D models and the 3-D elastic model.

13.53 15

However, large deflections in comparison to the other approaches appear for the elasto-plastic and hypoplastic models used. It is immediately emphasized that the calibration procedure based on laboratory tests involves softer results than those issued from the more empirical procedure.

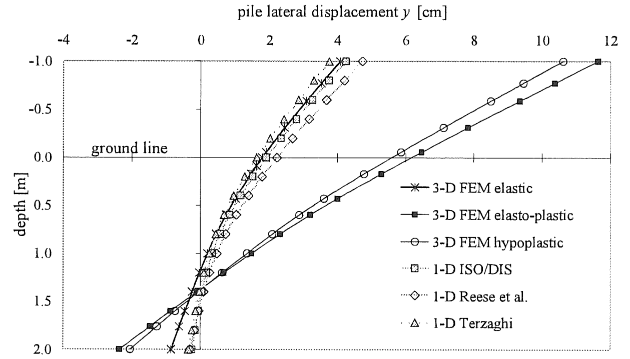

Fig. 7. Pile deflection distribution along the depth for all methods

The results reveal that the pile lateral displacement at ground line for the elastic model assuming a pile-soil interaction with frictional behavior and possible separation reaches 1.8 cm. Compared to the result obtained with the pile and soil entirely connected (1.0 cm), a difference of 80 % is observed which clearly emphasizes the important effect of a refined pile-soil interaction (frictional behavior and separation).

Comparison between 3-D elastic analyses with $E = 2.35$ MPa and the 3-D elasto-plastic model with $E = 4.4$ MPa (ratio of about 2 between the initial stiffness) reveals the importance of the plastic development in the lateral pile behavior. Fig. 9 shows the distribution of the plastic region after loading in the case of the 3-D analysis with the elasto-plastic model. The two failure mechanisms, i.e. the wedge failure and the plastic flow failure as proposed by Reese et al. (1974) are well highlighted. The transition however takes place at about 1.3 m depth while this depth should be 0.7 m according to Reese et al. (1974). The shape of the wedge mechanism is characterized by angles β_G of about 50° and 20° in the passive and the active region. The shape of the wedge is in relative good agreement with the Rankine theory ($\beta_G = \pi/4 + \varphi'/2 = 61°$ and $\beta_G = \pi/4 - \varphi'/2 = 28°$ for passive and active regions, respectively).

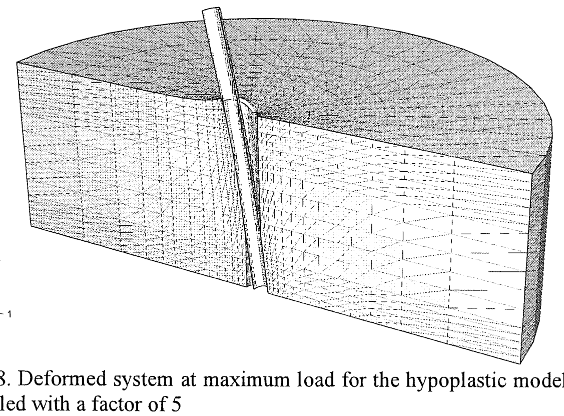

Fig. 8. Deformed system at maximum load for the hypoplastic modeled – scaled with a factor of 5

Fig. 10 depicts the void ratio distribution e for the hypoplastic case at maximum load. In the area close to the surface a decrease of the void ratio can be clearly identified. The extent of the depth (0.7 m) of the failed zone is in better agreement with empirical observations made by Reese et al. (1974) that the elasto-plastic model

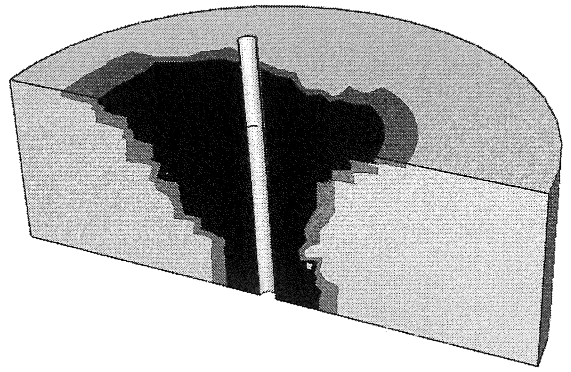

Fig. 9. Plastic region at lateral loading of 10 kN for the elasto-plastic model.

The p-y curves derived from three of the investigated methods are plotted in Fig. 11 up to a lateral load of 10 kN. It can be seen that the small strain stiffness (initial slope of the curve) for the 3-D analysis with elasto-plastic model is constant with the depth while the 1-D approach and hypoplastic model capture an increasing initial stiffness. Consequently, according to the elasto-plastic model the soil behaves more stiffly near the ground surface while it behaves more softly at depth. On the other hand, the increasing rate of the stiffness is smaller for the hypoplastic model than for the subgrade reaction procedure.

It can be seen in Fig. 11 that the subgrade reaction approach underestimates the ultimate lateral reaction for small depths while it seems to overestimate them for greater depths compared to the 3-D model. However, it is difficult to draw conclusions for deeper layers where the lateral displacements are limited. Note that the asymptotical value of the p-y curves for the subgrade reaction approach for $z = 176$ cm is about 120 kN/m. The ultimate lateral reactions for the hypoplastic and elasto-plastic model are in very good agreement

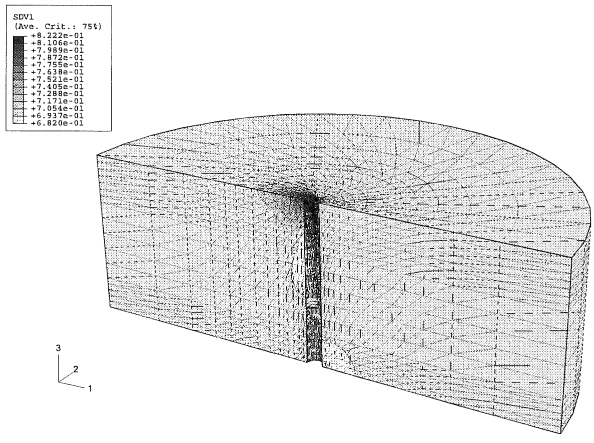

Fig. 10. Void ratio distribution e in the soil at 10 kN lateral load

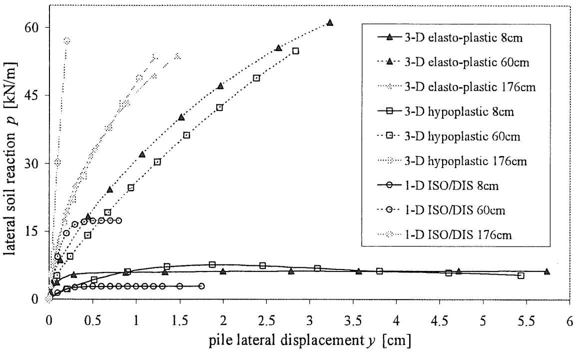

Fig. 11. *p-y* curves at different depths derived from 3-D and 1-D analyses

Figs. 6 and 7 reveal that the different 1-D empirical approaches are in good agreement with each other. In addition, the 3-D elastic model calibrated based on the Terzaghi's recommendations provides similar results with the 1-D approaches. Figs. 6, 7 and 11 also show the very good correspondence between the 3-D analysis using a simple elasto-plastic model and a more elaborated hypoplastic model since both the pile deflection and the ultimate soil resistance are similar. This match was expected since the calibration of the elastic and strength parameters for these two latter models are based on the same laboratory tests. Consequently this good agreement emphasizes the calibration procedure adopted. However, important differences with the 1-D approaches are depicted for both the deflection and the soil resistance. It should be emphasized that the absolute and relative differences of the pile displacements decrease for a factor of safety equal to 3 (Table 5).

In order to explain this difference, it should be first noted that the laboratory tests performed by Vanden Berghe (2001) did not focus on small confining pressures. This means that the soil behavior, corresponding to low mean pressures σ_m developed in the investigated reference case, might not have been accurately captured by the extrapolation using the power approximation (Eq. 10) and thus lead to an inaccuracy in the secant Young's modulus estimation for the elasto-plastic model. For the hypoplasticity a smaller secant stiffness of the system for small confining pressures was found amongst others by Wiemann et al. (2004). In addition, if our reference case implies a reduced scale geometry with small confining pressures, the 1-D approaches are mainly derived from full-scale laterally loaded tests where significantly higher mean pressures occur.

The large displacements for the approach applying the hypoplasticity and the elasto-plastic model arise presumably also from neglecting the loading history and therefore the missing "memory" of the imposed material law. The two models are calibrated with reconstituted laboratory samples carried out in order to obtain an initial void ratio of 0.7. But since a completely undisturbed soil which has not been loaded is rather improbable to encounter, specially around the pile, the simple material models as those used in the 1-D approach tend to cover general, load history independent problems. For the investigated case and the deflections given in Fig. 7 this could imply that the pile modeled in combination with the hypoplastic or elasto-plastic soil models react too softly in comparison to the other models because the load history (e.g. pile installation effects) is neither known nor taken into account. For example, an initial void ratio e_0 of 0.55 instead of 0.7 for the investigated hypoplastic model leads to a maximum deflection at the pile head of 3.9 cm instead of 10.3 cm, i.e. a decrease of more than 60 % of the lateral displacement. This example highlights the importance of the installation effect.

Beside the soil parameters, the interface parameters affect the pile response. In this investigation, a frictional behavior has been considered with a wall friction angle $\delta = 0.5\varphi'$. Some numerical analyses using the elasto-plastic model indicate that a change of the angle of interface friction δ from $0.5\varphi'$ to $0.8\varphi'$ involves a decrease of about 10 % of the lateral displacement.

Table 5. Results summary

approach	type	$k(z)$ or $E(z)$	p-y or q-ε_1	contact	y_{max} # FS=1.4 [cm]	y_{GL} ## FS=1.4 [cm]	y_{max} FS=3 [cm]
Terzaghi	1-D			*NA*	3.8	1.6	1.7
constant reaction	1-D			*NA*	3.8	1.6	1.7
API	1-D			*NA*	4.2	1.9	1.3
Reese et al.	1-D			*NA*	4.7	2.2	1.5
analytical solution	3-D			*CC*	3.3	1.3	1.5
linear elastic	3-D			*CC*	2.7	1.0	1.3
linear elastic	3-D			*F+S*	4.1	1.8	1.8
elasto-plastic	3-D			*F+S*	11.6	6.2	2.7
hypoplastic	3-D			*F+S*	10	5.6	3.2

\# *FS is the factor of safety*

\## y_{GL} *is the lateral displacement a ground line*

NA = not applicable

CC = completely connected

F+S = frictional behavior with possible separation

CONCLUSIONS AND OUTLOOK

The main objective of the present paper was to compare the most commonly used methods for simulating the lateral behavior of piles for a reference case. The comparison of the displacements is only valid for the problem analyzed: conclusions could vary depending on the scale of the sample problem, on the intensity of the lateral load and on the level at which displacements are compared. Nevertheless, some general conclusions can be drawn. Both 1-D subgrade reaction approaches and more complex 3-D analyses modeling the soil as a continuum have been investigated.

For the comparison, a careful choice of parameters is first conducted. While the subgrade reaction method requires only a small number of parameters, complexity arises when calibrating the 3-D models since the number of parameters increases highly. Two wide categories of design procedures have been applied. On one hand, the parameters evaluation based on empirical relationships for cohesionless sand and representing the engineering practice was used for the 1-D approaches and the 3-D approach with the elastic model. On the other hand the parameters for more complex models required the use of carefully conducted triaxial testing, paying special attention to the initial void ratio and the stress range implied by the loading in the representative soil's working zone. In this way laboratory investigations on Brusselian sand considering simple geostatic conditions to define the stress range were adopted for the elasto-plastic and hypoplastic models.

In addition to the continuum definition (soil and pile), the contact

definition requires great attention.
The validity of the 3-D model was confirmed by the analytical solution based on Mindlin's closed form solution. The elastic analysis allows to highlight the important effect of the pile-soil separation for a laterally loaded pile.
The calculations reported herein highlight the following points. The different approaches lead to two different results. It was indeed found good agreement between methods calibrated with the same strategy. However, the methods calibrated based on laboratory tests seem to behave more softly than the other approaches in spite of their increased complexity. Several reasons have been suggested with a view to explain the difference between the methods. The softer behavior estimated by more complex models could presumably be due to the low stress level implied in the reference case and due to the lack of accounting for the load history (pile installation effect). The presented calculation results deal indeed with a sample problem of unusually small scale, compared to the scale at which the pragmatic design methods have been validated. This comparison calls for experimental validation in order to see which approach is adequate. Reduced scale tests, implying sand pluviation around the pile, are planned to verify the theoretical findings from the parameter definition and the numerical studies.
The findings stress the importance of the designer's experience and the need to calibrate the approaches with test observations. Attempts to design a well mastered problem using potentially more powerful and versatile methods require extreme care. Difficulties arise because comparable results could only be obtained by selecting deformation parameters at the same mobilization ratio (inverse of the factor of safety).

ACKNOWLEDGEMENTS

The work presented herein forms part of the project "ETIB - Enhanced Economy of Tubular Piles by Improved Buckling Design" supported by the Research Fund for Coal and Steel of the European Commission (contract number RFS-CR-04041, period 01/07/04 – 01/07/07). The work performed is the result of close cooperation with the following project members: Alex Schmitt and Marc Meyrer (ProfilARBED), Hannu Jokiniemi (Rautaruukki), Emmanuel Bortolotti (RDCS), Nicolas Charue (Université catholique de Louvain). The authors are grateful for their support and the cooperation.
The authors wish also to thank the Belgian National Fund for Scientific Research FRIA, which granted Olivier Tomboy a Research Fellowship.

REFERENCES

API (1994) Recommended Practice 2A-LRFD (RP2A-LRFD) "Recommended Practice for Planning, Design and Constructing Fixed Offshore Platforms - Load and resistance Factor Design".

Baguelin, F., Frank, R., Saïd, Y.H. (1977). "Theoretical study of lateral reaction mechanism of piles", *Géotechnique*,Vol 27,No 3,pp 405-434.

Bauer, E. (1996)."Calibration of a comprehensive hypoplastic model for granular material", *Soils and Foundations*, Vol 36, No 1, pp 13-26.

Bauer, E., Herle, I. (2000). "Stationary states in hypoplasticity", *Constitutive Modelling of Granular Materials*, Ed. Kolymbas D., Springer, pp. 167-192.

Chambon, R., Renoud-Lias, B. (1979), "Incremental non-linear stress-strain relationship for soil and integration by FEM", Wittke, W. (Ed.), *3rd Int. Conf. on Numer. Methods in Geomech.*, pp. 1309–1332.

Charue, N., Holeyman, A., Hübner, A., Saal, A., Tomboy, O. (2006) "Design, build up and control of a large scale experimental set-up for laterally and vertically loaded piles in dry sand", *ISOPE conference*, San Francisco.

Dahlhoff, P., Steck, M., Taferner, J. (2003). "Chancen und Grenzen von Monopiles – Erste Erkenntnisse aus dem Forschungsvorhaben Opti-Pile", Chancen und Grenzen von Monopiles, *2. Tagung Offshore Windenergie*.

Darve, F. (1974). "*Contribution à la détermination de la loi rhéologues incrémentelale des sols*", Université Scientifique et Médicale de Grenoble, Doctoral Thesis.

Det Norske Veritas (2004). DNV-OS-J101. "Design of offshore wind turbine structures".

Grabe, J., Dührkop, J., Mahutka, K.-P. (2005). "Monopilegründungen von Offshore Windenergieanlagen - Zum Ansatz der Bettung", *Bautechnik*, Vol 82, No 1.

Gudehus, G. (1996). "A comprehensive constitutive equation for granular materials", *Soils and Foundations*, Vol 36, No 1., pp 1–12.

Herle, I., Gudehus, G. (1999). "Determination of parameters of a hypoplastic constitutive model from properties of grain assemblies", *Mechanics of cohesive-frictional materials*, No 4, pp 461-486.

Heteneyi, M. (1946). "Beams on elastic foundations", Ann. Arbor, Mich, The University of Michigan Press.

Hibbit, H.D, Karlsson, B.G., Sorensen (2005). "ABAQUS Theory Manual", Version 6.5.

ISO/DIS 19902 (2004). "Petroleum and Natural Gas industries – Fixed Steel Offshore Structures", Submitted version on 2004.

Khulaway, F.H. (1991). "*Drilled shaft foundations*". Foundation engineering handbook, Eds H.Y. Fang, Van Nostrand Reinhold, New York.

Kolymbas, D. (1988). "*Eine konstitutive Theorie für Böden und andere körnige Stoffe*", Habilitation, Karlsruhe, Veröffentlichung des Instituts für Bodenmechanik und Felsmechanik an der Universität Fridericiana in Karlsruhe, Vol 109, Karlsruhe.

McClelland, B, Focht, J.A. (1956). "Soil modulus for laterally loaded piles", *Journal of the soil mechanics and foundations division, ASCE*, Vol 101, pp 1049–1063.

Poulos, H.G. (1971). "Behaviour of laterally loaded piles : 1 - Single piles". *Journal of the soil mechanics and foundations division* , ASCE, Vol 97, pp 711-731.

Poulos, H.G., Davis, E.H. (1980). "*Pile foundation analysis and design*", Series in geotechnical engineering, Eds. T.W. Lambe, R.V. Whitman, John Wiley and sons.

Reese, L.C., Cox, W.R., Kopp, F.D. (1974). "Analysis of Laterally Loaded Piles in Sand", *Offshore Technologie Conference*, Dallas Texas, paper OTC 2080.

Reese, L.C., Van Impe W.F. (2001). "*Single piles and pile groups under lateral loading*", A.A. Balkema, Rotterdam.

Terzaghi K (1955). "Evalution of coefficients of subgrade reaction". *Geotechnique,* Vol 5 , 297–326.

Truesdell, C. (1955). "Hypo-elasticity". *J. Rational Mech. Anal.*, Vol 4, pp 83–133.

Vanden Berghe, J.-F. (2001). "*Sand Strength degradation within the framework of vibratory pile driving*". Doctoral Thesis, Université Catholique de Louvain.

Wiemann, J., Lesny, K., Richwien, W. (2002). "Gründung von Offshore – Windenergieanlagen – Gründungskonzepte und geotechnische Grundlagen". *Mitteilungen - Grundbau und Bodenmechanik der Universität Essen*, Vol 29, Verlag Glückauf, Essen.

Wiemann, J., Lesny, K., Richwien, W. (2004). "Anwendbarkeit von Standardverfahren zur Bemessung von Pfahlgründungen für Offshore-WEA". *3. Symposium Offshore-Windenergie Bau- und umwelttechnische Aspekte*, Hannover.

Winkler, E. (1867). "Die Lehre von Elastizität und Festigkeit", Prague, H Dominikus.